AD-A261 846

ICASE

A NEW DIRECTION IN HYDRODYNAMIC STABILITY: BEYOND EIGENVALUES

Lloyd N. Trefethen
Anne E. Trefethen
Satish C. Reddy
Tobin A. Driscoll

DTIC
S ELECTE
MAR12 1993
E D

NASA
National Aeronautics and
Space Administration
Langley Research Center
Hampton, Virginia 23665-5225

93-05247

93 3 11 077

A NEW DIRECTION IN HYDRODYNAMIC STABILITY: BEYOND EIGENVALUES

Lloyd N. Trefethen[1], Anne E. Trefethen[2], Satish C. Reddy[3], Tobin A. Driscoll[4]

ABSTRACT

Fluid flows that are smooth at low speeds become unstable and then turbulent at higher speeds. This phenomenon has traditionally been investigated by linearizing the equations of flow and looking for unstable eigenvalues of the linearized problem, but the results agree poorly in many cases with experiments. Nevertheless, it has become clear in recent years that linear effects play a central role in hydrodynamic instability. A reconciliation of these findings with the traditional analysis can be obtained by considering the "pseudospectra" of the linearized problem, which reveal that small perturbations to the smooth flow in the form of streamwise vortices may be amplified by factors on the order of 10^5 by a linear mechanism, even though all the eigenmodes are stable. The same principles apply also to other problems in the mathematical sciences that involve non-orthogonal eigenfunctions.

DTIC QUALITY INSPECTED 8

Accesion For		
NTIS CRA&I		☒
DTIC TAB		☐
Unannounced		☐
Justification		
By		
Distribution /		
Availability Codes		
Dist	Avail and / or Special	
A-1		

Contents

Introduction

A change of paradigm is taking place in the field of hydrodynamic stability. This is the field devoted to the study of how laminar fluid flows become unstable, the precursor to turbulence (1, 2). It is well known that turbulence is an unsolved problem, but not so well known that despite the efforts of generations of applied mathematicians beginning with Stokes, Kelvin, Rayleigh, and Reynolds a century ago, many of the presumably simpler phenomena of hydrodynamic stability also remain ill-understood (3).

The traditional paradigm is eigenvalue analysis:

> I. Linearize about the laminar solution;

> II. Look for unstable eigenvalues of the linearized problem.

An "unstable eigenvalue" means an eigenvalue in the complex upper half-plane, corresponding to an eigenmode of the linearized problem that grows exponentially as a function of time t. It is natural to expect that a flow will behave unstably *if and only if there exists such a growing eigenmode, and over the* years a great deal of knowledge has been obtained about which flows possess such modes, a distinction that depends on the geometry, the Reynolds number, and sometimes other parameters.

For some flows, the predictions of eigenvalue analysis match laboratory experiments. Examples are Rayleigh-Bénard convection (a stationary fluid heated from below) and Taylor-Couette flow (between a stationary outer and a rotating inner cylinder). For other flows, the predictions of eigenvalue analysis fail to match most experiments. In this article we consider the two most extensively studied examples of this kind: (plane) Couette flow, the flow with a linear velocity profile between two infinite flat plates moving parallel to one another, and (plane) Poiseuille flow, the flow with a parabolic velocity profile between two stationary plates (Fig. 1). Other examples where eigenvalue analysis fails include pipe Poiseuille flow (in a cylindrical pipe) and, to a lesser degree, Blasius boundary layer flow (near a flat wall).

For Poiseuille flow, eigenvalue analysis predicts a critical Reynolds number (4) $R = 5772.22$ at which instability should first occur (5), but in the laboratory, transition to turbulence is observed at Reynolds numbers as low as $R \approx 1000$ (6).
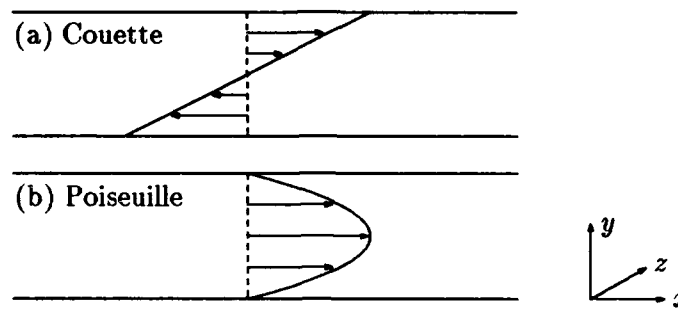
Fig. 1. Velocity profiles for the two laminar flows considered in this article (independent of x and z). The geometry is an infinite 3D slab of viscous incompressible fluid bounded by parallel walls. The laminar solutions satisfy the Navier-Stokes equations for all Reynolds numbers R, but for higher R the flows are unstable and rapidly become turbulent.

For Couette flow, eigenvalue analysis predicts stability for all R, but transition is observed for Reynolds numbers as low as $R \approx 350$ (7). These anomalies of "subcritical transition to turbulence" have been recognized for many years, and the explanation has usually been attributed to step I above. If linearization has failed, the reasoning goes, one must look more closely at the nonlinear terms, or perhaps linearize about a solution other than the laminar one (the theory of "secondary instability" (8, 9)).

Recently it has emerged, however, that the failure of eigenvalue analysis may more justly be attributable to step II. It is a fact of linear algebra that even if all of the eigenvalues of a linear system are distinct and lie well inside the lower half-plane, inputs to that system may be amplified by arbitrarily large factors if the eigenfunctions are not orthogonal. A matrix or operator whose eigenfunctions are orthogonal is said to be *normal* (10, 11). The linear operators that arise in the Bénard and Taylor-Couette problems are normal or close to normal. By contrast Reddy, Schmid and Henningson discovered in 1990 that the operators that arise in Poiseuille and Couette flow are in a sense exponentially far from normal (12). At about the same time the startling discovery was made by Gustavsson (13) and Henningson (14) and independently by Butler and Farrell (15) that small perturbations to these flows may be amplified by factors of many thousands, even when all the eigenvalues are in the lower half-plane. The paper by Butler and Farrell is an important and elegant one. It discusses many details omitted here, and together with a related more recent paper by
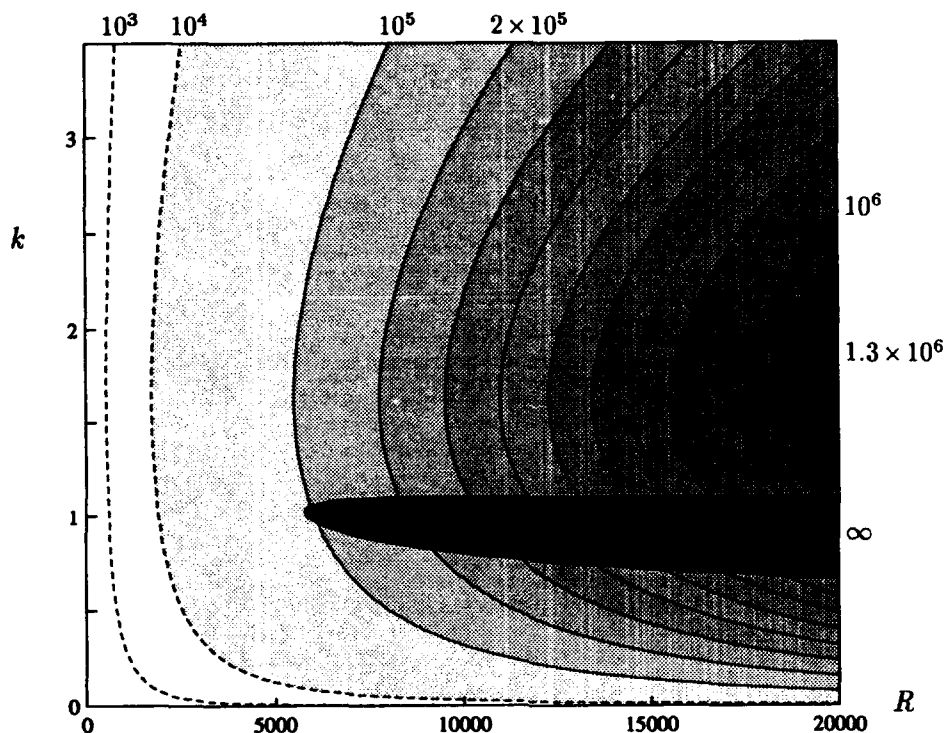
Fig. 2. Maximum possible amplification of 3D perturbations in linearized Poiseuille flow as a function of Reynolds number R and x-z wave number magnitude $k = \sqrt{\alpha^2 + \beta^2}$. In the black region, with leftmost point $R = 5772$, unstable eigenmodes exist and unbounded amplification is possible. The contours outside that region correspond to finite amplification factors of 10^3, 10^4 (dashed), and $1 \times 10^5, 2 \times 10^5, \ldots, 1.3 \times 10^6$. For example, amplification by a factor of 1000 is possible for all $R \geq 549$. In the laboratory, transition to turbulence is observed at $R \approx 1000$. The analogous picture for Couette flow looks qualitatively similar except that there is no black region.

Reddy and Henningson (16), it forms the foundation of the present work (17).

Fig. 2 illustrates these factors of thousands. The black region has appeared in many papers and books and corresponds to parameters for which unstable eigenmodes exist (18). The contours defining the shaded regions are new and quantify the non-modal amplifications that may occur in these flows. (A precise explanation of this plot is given in the next section.) The possibility of amplification of perturbations of viscous flows by non-modal linear mechanisms has been recognized for a century (19–23), but until the recent developments, it was not known that the magnitudes involved were huge.

An essential feature of the amplification process of Fig. 2 is that it acts upon 3D perturbations of the laminar flow field. In much of the theoretical literature of hydrodynamic stability, attention has been restricted to 2D (x-y) perturbations, and in particular, the well-known Orr-Sommerfeld equation is an eigenvalue equation for 2D perturbations. A principal justification for this restriction has been Squire's theorem of 1933, which asserts that if a flow has an unstable 3D eigenmode for some R, then it has an unstable 2D eigenmode for some lower value of R (24). The new results indicate that this emphasis on 2D perturbations has been misplaced. When only 2D perturbations are considered, amplification is still possible, but far weaker.

This emphasis on 3D, *linear but non-modal* effects is the emerging new paradigm in hydrodynamic stability.

Streamwise vortices and streaks

The flow features associated with this amplification process have a distinctive form (Fig. 3):

Input: *streamwise vortex,*

Output: *streamwise streak.*

A streamwise vortex is an elongated region of vorticity approximately aligned with the x axis, and a streamwise streak is an elongated region of high or low velocity (relative to the mean flow) approximately in the x direction. Streamwise vortices and streaks are persistent features in laboratory experiments involving all kinds of internal and boundary layer shear flows (25). Physically, they are not hard to explain: in a shear flow, a small perturbation in the form of a streamwise vortex may move fluid from a region of higher to lower x velocity, or vice versa, where it will appear as a large local perturbation in the x velocity (26). Since these features constitute 3D perturbations of the flow field, however, their prevalence has been difficult to reconcile with the predictions of eigenvalue analysis. Non-modal analysis offers a resolution of this difficulty, for although streamwise streaks are not eigenmodes of the linearized flow problem, they are *pseudomodes.*

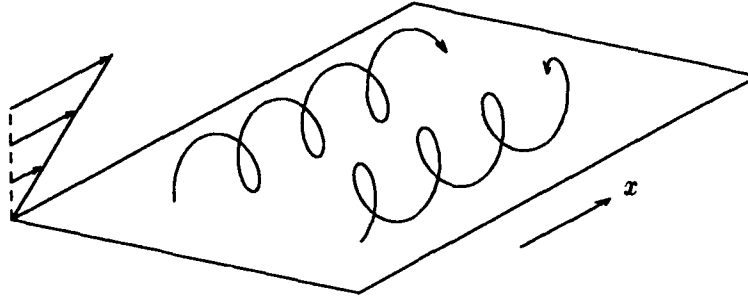To explain this term and our use of the words "input" and "output," we

Fig. 3. Schematic illustration of a structure that appears in many shear flows. A low-amplitude vortex or counter-rotating pair of vortices roughly aligned with the flow entrains fluid from regions of high to low x velocity and vice versa. The entrained fluid appears as a streak of locally high or low streamwise velocity (not shown). This process is linear, but unrelated to eigenmodes.

must define the evolution operator that is the mathematical basis of this article. Let $u_0 = u_0(x,y,z)$ denote the vector velocity field corresponding to Poiseuille or Couette laminar flow (Fig. 1). Let $u_0 + \mathbf{u}(t) = u_0(x,y,z) + \mathbf{u}(x,y,z,t)$ be the velocity field of a slightly perturbed flow, i.e., a nearby solution to the Navier-Stokes equations. (We use bold face letters to distinguish quantities that are functions of t.) If we take $\mathbf{u}$ to be infinitesimal, then it satisfies an equation

$$\frac{d\mathbf{u}}{dt}(t) = -i\mathcal{L}\mathbf{u}(t),$$

where $\mathcal{L}$ is a linear operator that we call the *linearized Navier-Stokes evolution operator*. (The factor $-i = -\sqrt{-1}$ is a matter of convention.) As a measure of the size of solutions to this equation we define

$$\|\mathbf{u}(t)\| = \left(\int |\mathbf{u}(x,y,z,t)|^2 dx\,dy\,dz \right)^{1/2},$$

which we call the *energy norm* since its square corresponds to energy.

Suppose now that the linearized fluid system is driven by a signal of the form $\mathbf{v}(t) = e^{-i\omega t}v$ for some frequency $\omega \in \mathbb{C}$ and function $v = v(x,y,z)$:

$$\frac{d\mathbf{u}}{dt}(t) = -i\mathcal{L}\mathbf{u}(t) + e^{-i\omega t}v, \quad -\infty < t < \infty.$$

It is easily verified that the response will be

$$\mathbf{u}(t) = ie^{-i\omega t}u, \qquad u = (\omega I - \mathcal{L})^{-1}v,$$

where I denotes the identity operator. Thus the operator $(\omega I - \mathcal{L})^{-1}$, known as the *resolvent* of $\mathcal{L}$, transforms "inputs" v to the linearized fluid flow at frequency ω into corresponding "outputs" u (10, 11). The degree of amplification that may occur in the process is equal to the operator norm

$$\|(\omega I - \mathcal{L})^{-1}\| \overset{\text{def}}{=} \sup_{v \neq 0} \frac{\|u\|}{\|v\|}.$$

Since an arbitrary time-dependent perturbation of the laminar flow can be reduced to an integral over real frequencies by Fourier analysis, values of ω on the real axis are of particular interest. The maximum possible amplification over all real frequencies is $\sup_{\omega \in \mathbb{R}} \|(\omega I - \mathcal{L})^{-1}\|$, and this is the quantity plotted in Fig. 2.

An eigenvalue of $\mathcal{L}$ is a number $\omega \in \mathbb{C}$ such that $\mathcal{L}u = \omega u$ for some corresponding eigenfunction u. Equivalently, it is a number ω with the property that inputs with frequency ω can be amplified unboundedly: $\|(\omega I - \mathcal{L})^{-1}\| = \infty$. More generally, for any $\epsilon \geq 0$, an *ϵ-pseudo-eigenvalue* of $\mathcal{L}$ is a number ω such that $\|(\omega I - \mathcal{L})^{-1}\| \geq \epsilon^{-1}$, and a corresponding *$\epsilon$-pseudo-eigenfunction* or *ϵ-pseudomode* is any function u with $\|\mathcal{L}u - \omega u\| \leq \epsilon\|u\|$. If ϵ is very small, then an ϵ-pseudomode u may be excited to a substantial amplitude by a very small input, possibly including noise in an experimental apparatus. At $R = 5000$, for example, a streamwise streak is an ϵ-pseudomode of the linearized Poiseuille flow problem for $\epsilon \approx 1.2 \times 10^{-5}$ (Fig. 2) and thus can be excited by a streamwise vortex five orders of magnitude weaker in amplitude.

The set of ϵ-pseudo-eigenvalues of an operator is the *ϵ-pseudospectrum* (27):

$$\Lambda_\epsilon(\mathcal{L}) = \{\omega \in \mathbb{C} : \|(\omega I - \mathcal{L})^{-1}\| \geq \epsilon^{-1}\}.$$

The pseudospectra $\{\Lambda_\epsilon(\mathcal{L})\}$ form a nested family of sets in the complex plane, with $\Lambda_0(\mathcal{L})$ equal to the spectrum $\Lambda(\mathcal{L})$. If $\mathcal{L}$ is normal, $\Lambda_\epsilon(\mathcal{L})$ is the set of all points at distance $\leq \epsilon$ from $\Lambda(\mathcal{L})$, but in the non-normal case it may be much larger. The physical significance of pseudospectra can be described as follows. If a system is governed by a linear operator that is normal or close to normal—familiar examples include musical instruments, oscillating structures, and molecules as described by quantum mechanics—then the frequencies at which it resonates strongly are determined by its spectrum. The resonances of a system that is far from normal, however, can only be understood by examining its pseudospectra.

Spectra and pseudospectra

Figs. 4 and 5, the centerpieces of this article, depict spectra and pseudospectra for Couette flow at $R = 350$, 3500 and Poiseuille flow at $R = 1000$, 10000. These Reynolds numbers roughly span the range in each case from possible turbulence (in some experiments) to unavoidable turbulence (even in experiments under the most carefully controlled conditions). These and our other figures are the results of numerical computations. As a practical matter we first Fourier transform in x and z, reducing the calculation to one space dimension (y) and two real parameters α, β (wavenumbers in x, z). The generation of each figure then requires a minimization in the α-β plane (28).

Spectra of $\mathcal{L}_{\alpha\beta}$ for particular values of α and β have been published by various authors (5, 29), and pseudospectra of $\mathcal{L}_{\alpha\beta}$ will appear in (12, 16). Neither spectra nor pseudospectra of $\mathcal{L}$ itself have been plotted previously.

Fig. 4 reveals that in the case of Couette flow, the spectrum of $\mathcal{L}$ is a continuous region contained in the lower half-plane. (For each α, β pair the spectrum is discrete, but the union over α and β is a continuum, shown in the figure as a shaded region.) This is true for all R, corresponding to the unconditional stability of Couette flow according to eigenvalue analysis. The spectrum comes closest to the upper half-plane along the imaginary axis, at a distance $O(R^{-1})$ as $R \to \infty$. The pseudospectra of $\mathcal{L}$, by contrast, protrude significantly into the upper half-plane, indicating that evolution process governed by this operator will feature prominent non-modal effects.

One cannot see in Fig. 4 what values of α and β correspond to various points in the spectrum and pseudospectra. The situation is roughly as follows. The upper boundary of the spectrum corresponds to $\beta = 0$ and to values of α that grow in proportion to Reω. In the pseudospectra, the values of α are comparable but the values of β are $O(1)$. This difference in values of β reflects the fact that although the dominant eigenmodes of this problem are 2D, the dominant pseudomodes are 3D.

Fig. 5 reveals the more complicated situation for Poiseuille flow. The pseudospectra are qualitatively similar, again extending well into the upper half-plane (30). The boundary of the spectrum, however, is now determined by two

Fig. 4. Spectrum and ϵ-pseudospectra in the complex ω-plane of the linearized Navier-Stokes evolution operator for Couette flow at $R = 350$ and 3500. The spectrum is the shaded region, and the solid curves, from outer to inner, are the boundaries of the ϵ-pseudospectra with $\epsilon = 10^{-2}, 10^{-2.5}, 10^{-3}$, $10^{-3.5}$. The spectrum lies in the lower half-plane, but the pseudospectra extend significantly into the upper half-plane, revealing the non-normality of this operator. Note that the real and imaginary axes are scaled differently.

Fig. 5. Same as Fig. 4 but for Poiseuille flow with $R = 1000$, 10000. For $R > 5772$, two bumps in the spectrum extend into the upper half-plane. However, the large lobes of the pseudospectra along the imaginary axis are physically more important.

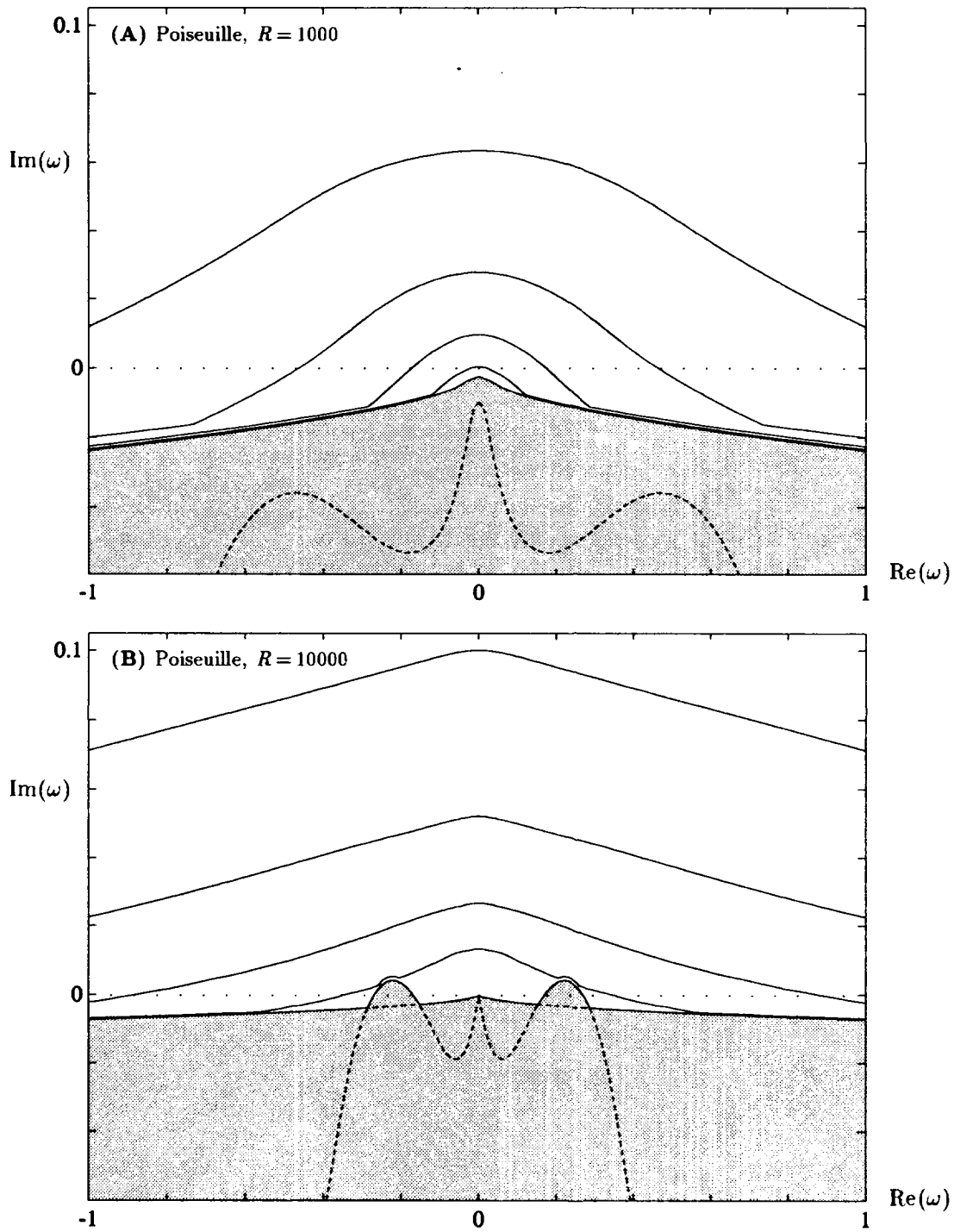distinct components, each with $\beta = 0$. One of these looks qualitatively like the boundary of the spectrum for Couette flow and corresponds to perturbations of the flow field that are symmetric about the centerline. The other is very different, consisting of bumps on either side of the origin corresponding to antisymmetric perturbations of the flow. For lower values of R, the spectrum is contained in the lower half-plane, but at $R = 5772$ the bumps cross the real axis. These bumps represent the mode that has received most of the attention in the literature, which is sometimes known as a Tollmien-Schlichting or TS wave. However, their negligible effect on the nearby pseudospectral contours reveals that this mode is oriented at a sizable angle to the remainder of the system (31). The pseudomodes associated with $\omega \approx 0$—streamwise streaks with $\alpha \approx 0$, $\beta \neq 0$—are physically more important.

We can summarize the implications of Figs. 4 and 5 by noting that whereas spectral analysis suggests that plane Couette and Poiseuille flows are fundamentally different, since one has unstable eigenmodes for certain values of R and the other does not, pseudospectral analysis suggests that they are fundamentally similar, as is observed in experiments.

Resonance curves

Figs. 6 and 7 represent slices of Figs. 4 and 5 along the real axis. In each figure $\|(\omega I - \mathcal{L})^{-1}\|$ is plotted as a function of $\omega \in \mathbb{R}$ for several values of R, indicating the factors by which linearized Couette and Poiseuille flows are capable of amplifying time-dependent perturbations at various real frequencies. When the amplification is large we speak of the phenomenon of resonance, although a more careful term might be "pseudo-resonance."

For Couette flow, no significant resonance is present except near $\omega = 0$. There, the amplification may be powerful indeed, reaching a value $\mathcal{O}(R^2)$ although the spectrum lies at a distance $O(R^{-1})$ below the real axis. For Poiseuille flow, the behavior for $\omega \approx 0$ is similar, but for $R > 5772$ an additional resonance for larger ω appears due to the unstable eigenmode. In principle, this mode would dominate if one could set up an experiment involving a sufficiently long channel and a sufficiently smooth flow. Under conditions where this can happen, however, low-frequency inputs are already subject to non-modal amplification by a factor of order 10^5.
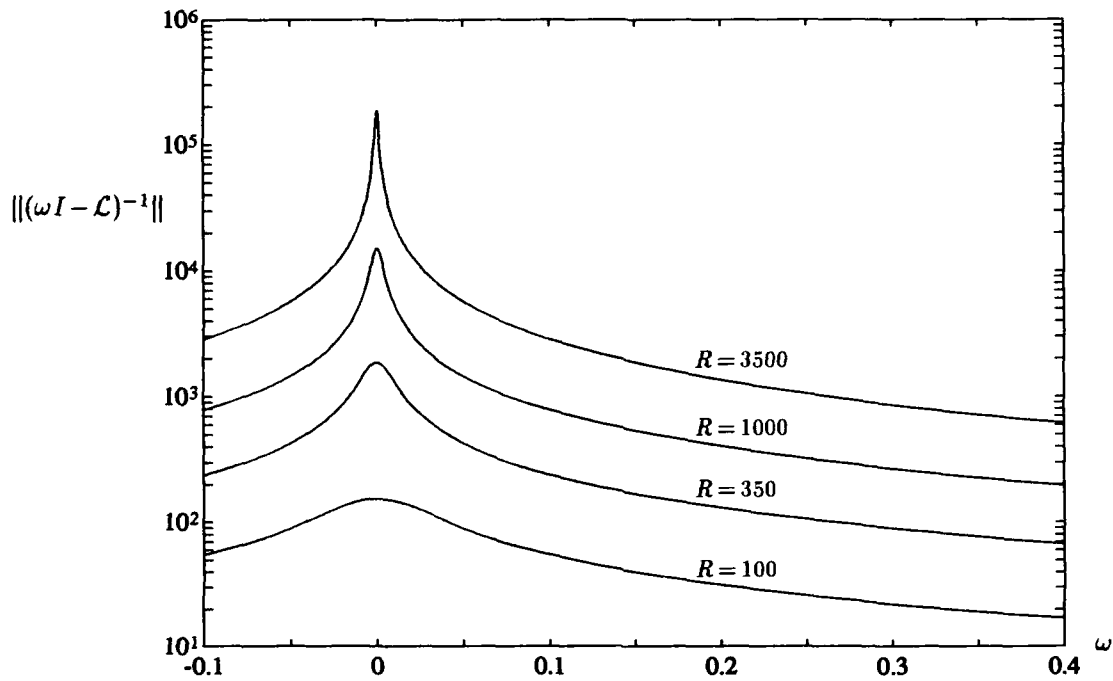
Fig. 6. Resonance or "pseudo-resonance" curves for Couette flow. Each curve shows $\|(\omega I - \mathcal{L})^{-1}\|$, the maximum possible amplification of perturbations to the laminar flow field at frequency ω.
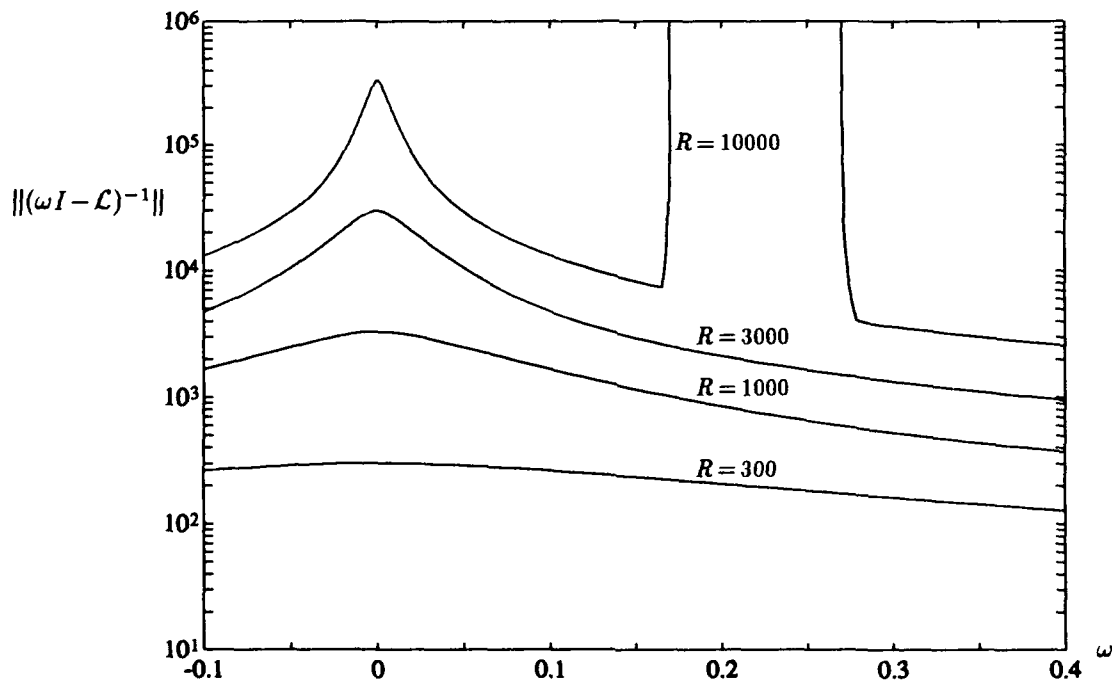

Fig. 7. Like Fig. 6 but for Poiseuille flow. For $R > 5772$ infinite amplification is possible in principle, but of doubtful significance in practice.

Transient energy growth

Another aspect of linear, non-modal instability of fluid flows is the transient amplitude or energy growth that may evolve from certain initial conditions. This is the phenomenon that has been studied in the recent papers by Gustavsson, Butler and Farrell, and Reddy and Henningson, where many more physical details can be found.

Mathematically, consider the initial-value problem

$$\frac{d\mathbf{u}}{dt}(t) = -i\mathcal{L}\mathbf{u}(t), \quad t \geq 0, \quad \mathbf{u}(0) = v.$$

The solution can be written $\mathbf{u}(t) = \exp(-it\mathcal{L})v$, where $\exp(-it\mathcal{L})$ is the operator exponential. The factor by which such solutions can grow in time t is

$$\| \exp(-it\mathcal{L}) \| = \sup_{v \neq 0} \frac{\|\mathbf{u}(t)\|}{\|v\|},$$

and the energy growth is the square of this quantity. If $\mathcal{L}$ were a normal operator with spectrum in the lower half-plane, we would have $\| \exp(-it\mathcal{L}) \| \leq 1$ for all $t \geq 0$. In actuality, Gustavsson and Butler and Farrell discovered that the growth is $\| \exp(-it\mathcal{L}) \| = O(R)$, making the energy growth $O(R^2)$.

Fig. 8 illustrates this phenomenon for Couette flow at various Reynolds numbers. The agreement of the curves for finite R and $R = \infty$ can be explained as follows: the streamwise vortex/streak mechanism of energy growth is inviscid, and operates on a time scale $O(R)$ before being shut off by the effects of viscosity. Such behavior is physically straightforward, appearing complicated only when interpreted in the basis of eigenmodes.

Fig. 9 gives further information for Couette flow with $R = 350$; other Reynolds numbers are qualitatively similar. The restriction to x-independent flows ($\alpha = 0$) curtails the transient growth somewhat for small t but has no effect for larger t, when the maximal growth is achieved with $\alpha = 0$ anyway (i.e., a purely streamwise structure). The restriction to z-independent flows ($\beta = 0$), however, has a huge effect, shutting off most of the transient growth except for $t \approx 0$ (32).

The $O(R^2)$ resonances of Figs. 2,6,7 are approximately equal to the integrals under the curves in Figs. 8 and 9. Mathematically, this can be seen from

Amplitude $\|\exp(-it\mathcal{L})\|$

$R = \infty$

$R = 4000$

3500

3000

2500

2000

1500

1000

500

Energy $\|\exp(-it\mathcal{L})\|^2$

t

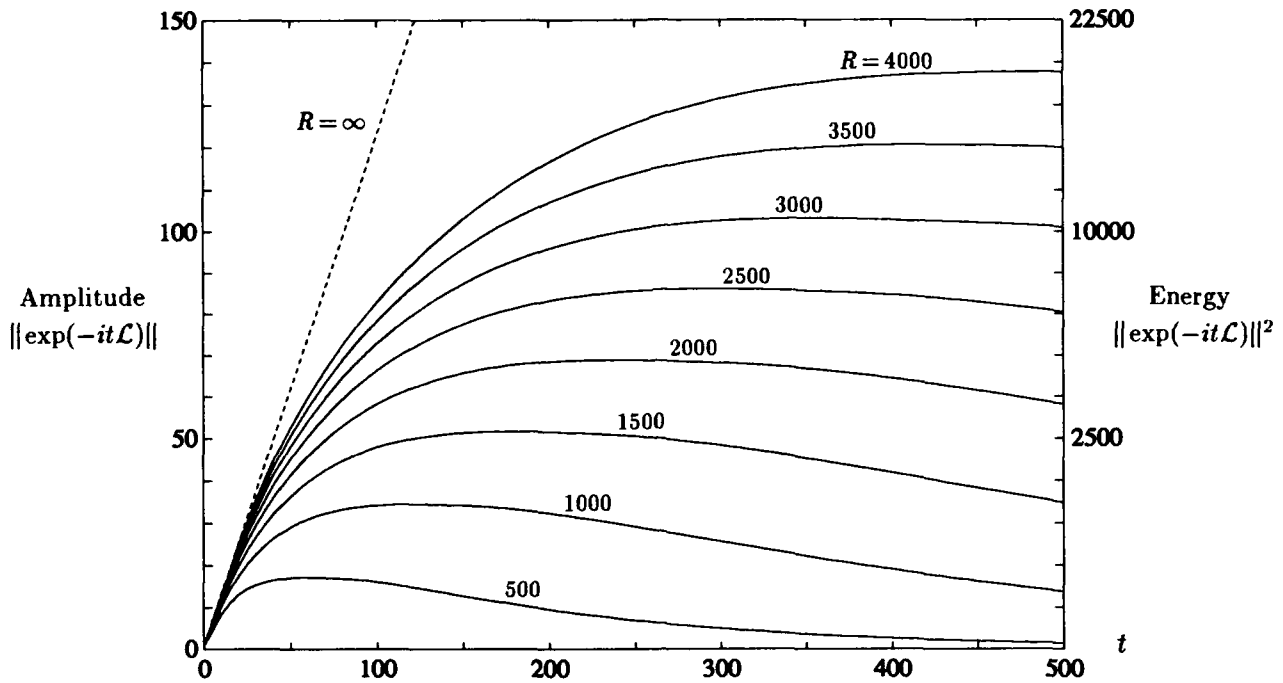**Fig. 8.** Non-modal transient energy growth for Couette flow. For any finite R, the effect of viscosity shuts off the growth on a time scale $O(R)$.

Amplitude $\|\exp(-it\mathcal{L})\|$

$\alpha = 0$

lower bound based on pseudospectra

$\beta = 0$ (2D)
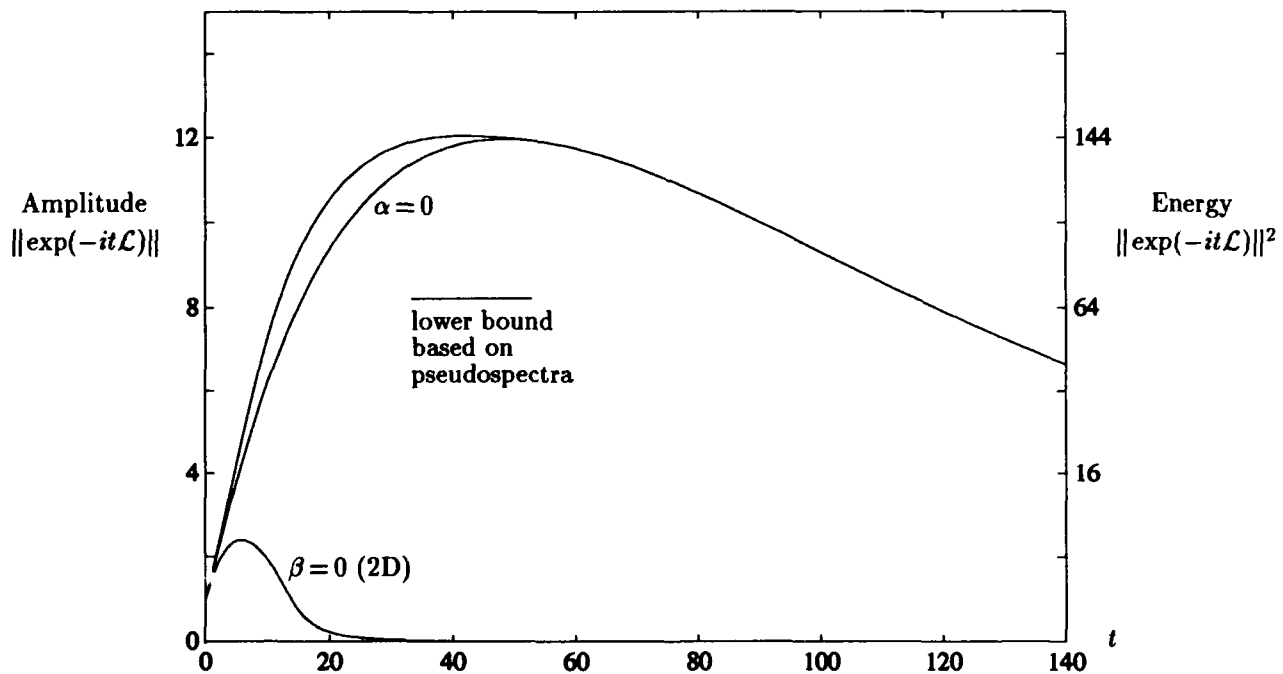
Energy $\|\exp(-it\mathcal{L})\|^2$

t

Fig. 9. Transient growth for Couette flow at $R = 350$. Little growth occurs when only 2D perturbations are allowed.
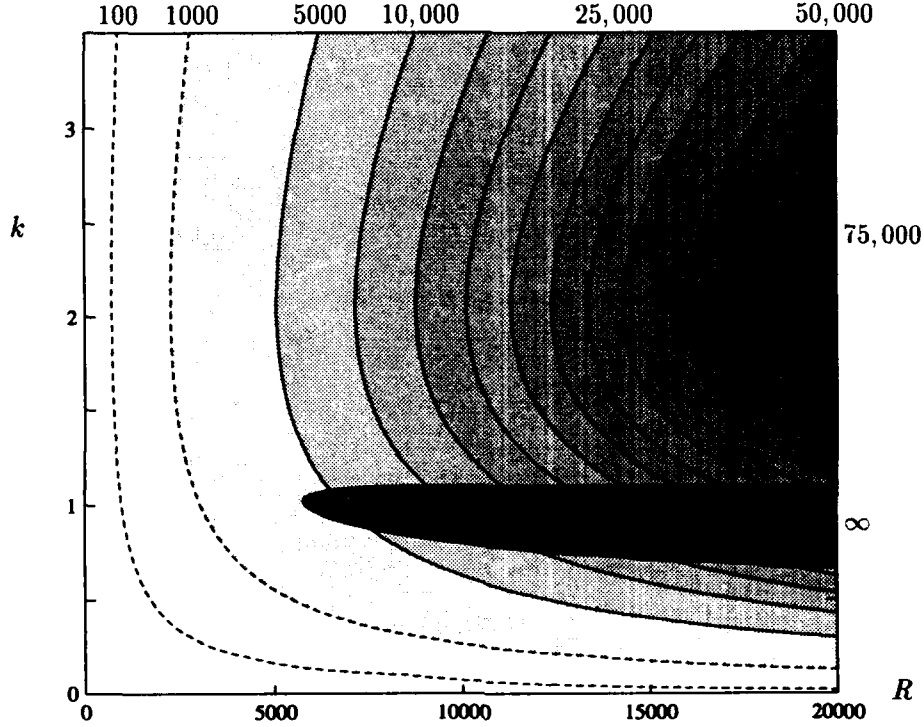
Fig. 10. Analogue of Fig. 2, showing transient energy growth factors $\sup_{t\geq 0} \|\exp(-it\mathcal{L})\|^2$ instead of resonant amplification factors $\sup_{\omega\in\mathbb{R}} \|(\omega I - \mathcal{L})^{-1}\|$. For example, transient energy growth by a factor of 1000 is possible for all $R \geq 2260$. If $\mathcal{L}$ were normal, the growth factors would be exactly 1 outside the black region.

the formula $\mathcal{L}^{-1} = i\int_0^\infty \exp(-it\mathcal{L})\,dt$, which implies $\|\mathcal{L}^{-1}\| \leq \int_0^\infty \|\exp(-it\mathcal{L})\|\,dt$; in practice the inequality is typically within a factor of 2 of equality. We can interpret the $O(R^2)$ result physically by noting that the resonant amplification is due to a combination of two effects: one (normal) factor $O(R)$ representing the time scale over which input energy can accumulate before it eventually decays, and another (non-normal) factor $O(R)$ representing transient amplitude growth.

Analogues of Figs. 8 and 9 for Poiseuille flow look qualitatively the same; the differences for $R > 5772$ appear only for large t, off the scale of our plots. Fig. 10 is an analogue of Fig. 2 for the Poiseuille case that shows transient energy growth factors instead of resonance amplitudes (33).

A lower bound for transient growth factors can be derived from the geom-

etry of the pseudospectra in the complex upper half-plane. One can show:

$$\sup_{t\geq 0} \|\exp(-it\mathcal{L})\| \geq \sup_{\epsilon >0} \epsilon^{-1}\sigma_\epsilon(\mathcal{L}),$$

where $\sigma_\epsilon(\mathcal{L}) = \sup_{\omega\in\Lambda_\epsilon(\mathcal{L})}\mathrm{Im}\,\omega$ is the *ϵ-pseudospectral ordinate of $\mathcal{L}$* (11, 16). In words, if the pseudospectra protrude far into the upper half-plane, then substantial transient energy growth must be possible. The horizontal line segment in Fig. 9 marks this lower bound, which falls short of the true maximum by only about a factor of 1.4 in amplitude or 2.0 in energy, numbers typical of both Couette and Poiseuille flows for a wide range of R (3, 34).

Physically interesting pseudomodes

Instead of operator norms, it is customary in the literature to investigate the evolution of particular solutions chosen for one physical reason or another. The amplitude history of the solution with initial flow field $\mathbf{u}(0) = v$ is given by $\|\exp(-it\mathcal{L})v\|$, and the upper envelope of all such curves, corresponding to all initial functions v, is the operator norm $\|\exp(-it\mathcal{L})\|$ that we have discussed.

Three choices of v with particular claims to attention can be identified with the aid of the singular value decomposition (SVD), the natural tool for all kinds of questions involving norms and extrema of nonsymmetric matrices and operators (35). Fig. 11 displays the curves $\|\exp(-it\mathcal{L})v\|$ corresponding to the principal right singular vectors of the following operators:

$v_1:$ $\exp(-i0^+\mathcal{L})$ (maximal initial growth rate),

$v_2:$ $\exp(-it_{\mathrm{opt}}\mathcal{L})$ (maximal total growth),

$v_3:$ $\mathcal{L}^{-1}$ (maximal resonance).

The function v_1 is the perturbation with maximal growth rate at $t = 0$, a function that has been studied by Serrin, Busse, Joseph, Lumley, and others (2, 8, 15, 36). (The notation $\exp(-i0^+\mathcal{L})$ indicates the limit of the SVD of $\exp(-it\mathcal{L})$ as $t \to 0$. A cleaner and computationally more appropriate characterization of the function v_1 is that it is the principal eigenfunction of $(\mathcal{L} - \mathcal{L}^*)/2i$, with growth rate at $t = 0$ equal to the corresponding eigenvalue, or equivalently, to the distance that the numerical range of $\mathcal{L}$ protrudes into the upper half-plane.) The function v_2 is the Butler-Farrell "optimal" that achieves maximal total

Fig. 11. Initial growth and eventual decay resulting from three particular initial perturbations v for Couette flow at $R = 350$. The dashed curve is the operator norm of Fig. 9.

growth at some time $t = t_{opt}$. The function v_3 is the one that excites a maximal resonant response in the sense of Figs. 2,6,7.

Fig. 11 reveals that although the physical ideas behind the functions v_1, v_2, v_3 are different, v_2 and v_3 at least lead to comparable energy growth. These functions are also similar in structure: both have approximately the form of streamwise vortices that evolve into streamwise streaks (corresponding to left rather than right singular vectors of the same operators). An analogous figure for Poiseuille flow looks roughly similar, but the gap between v_2 and v_3 is smaller and the gap between these and v_1 is larger.

The inviscid limit

The relationship between the stability theories for viscous and inviscid flows has been an awkward one (21). It is natural to expect that the mechanism of instability should be essentially inviscid, so that it should be possible to get at the essence of the matter by setting $R = \infty$, simplifying the equations greatly. Yet the results of inviscid stability analysis have generally matched neither the results of viscous analysis nor experimental observations. A conspicuous example is Rayleigh's theorem of 1880 (37), which asserts that unless the velocity profile contains an inflection point, an inviscid parallel shear flow is always stable, a conclusion plainly at odds with the observed behavior of Poiseuille and Couette flows at large finite Reynolds numbers.

We believe that much of the difficulty with the limit $R \to \infty$ has been due to misunderstanding of the significance of eigenvalues. Rayleigh's theorem, like Squire's theorem, is actually a statement about the existence of eigenvalues in the upper half-plane, and like Squire's theorem, it is mathematically correct but misleading. If one defines stability by energy growth instead of by eigenvalues, one finds that every planar shear flow with $R = \infty$ is unstable, regardless of the velocity profile. This observation is due to Ellingsen and Palm (38), with roots going back to Kelvin, and related results have been established by many others (23, 39). The example of Couette flow with $R = \infty$ and $\alpha = 0$ is particularly simple, for the equations reduce to the 2×2 block matrix problem

$$\begin{pmatrix} \hat{v} \\ \hat{\eta} \end{pmatrix}_t = \begin{pmatrix} 0 & 0 \\ -i\beta I & 0 \end{pmatrix} \begin{pmatrix} \hat{v} \\ \hat{\eta} \end{pmatrix},$$

where $\hat{v}$ and $\hat{\eta}$ represent the y components of velocity and vorticity (functions of y, after Fourier transformation in x and z). The matrix L in this equation is defective (i.e., nondiagonalizable), with $\| \exp(-itL) \| \sim Ct$ as $t \to \infty$ for some constant $C = C(\beta) < 1$ (after transformation to the energy norm). Thus inviscid Couette flow is linearly unstable, even though there is no exponentially growing eigenmode, which explains the dashed line in Fig. 8.

This "algebraic" instability of inviscid flows is well known among hydrodynamicists. What has been missing is a fully satisfactory link to the case of viscous flows, where the evolution operator is typically nondefective and eigenvalue analysis has been accepted as a test of stability. The point that has not

always been appreciated is that although a flow may be stable in the sense of bounded response to infinitesimal perturbations for each finite R, it does not follow that it satisfies any bound uniformly as $R \to \infty$. In the absence of a uniform bound, the notion of stability for large finite Reynolds numbers has little meaning (40).

Our computations indicate that by most measures, the limit $R \to \infty$ is a smooth one. Table 1 summarizes the behavior of a number of quantities in this limit and may serve as a reference point for most of our figures (41).

	Couette	α	β	Poiseuille	α	β
distance of spectrum from real axis	$(R/2.47)^{-1}$	0	0	$(R/2.47)^{-1}$	0	0
max. resonance $\sup_{\omega \in \mathbb{R}} \|(\omega I - \mathcal{L})^{-1}\|$	$(R/8.12)^2$	0	1.18	$(R/17.4)^2$	0	1.62
transient growth $\sup_{t>0} \|\exp(-it\mathcal{L})\|^2$	$(R/29.1)^2$	$35.7/R$	1.60	$(R/71.5)^2$	0	2.04
optimal time t_{opt}	$R/8.52$	”	”	$R/13.2$	”	”
lower bound based on pseudospectra	$(R/42.6)^2$	0	1.62	$(R/103.)^2$	0	2.04
transient growth $(\alpha = 0)$	$(R/29.3)^2$	0	1.66	$(R/71.5)^2$	0	2.04

Table 1. Leading-order behavior of various quantities as $R \to \infty$. These formulas are accurate to at least 1% for all $R > 100$. The results for Poiseuille flow pertain to the highly non-normal part of the problem, ignoring the $R > 5772$ mode (TS wave).

Destabilizing perturbations and secondary instability

There is an alternative, equivalent definition of the pseudospectra of an operator $\mathcal{L}$ (27, 42):

$$\Lambda_\epsilon(\mathcal{L}) = \mathrm{closure}\{\omega \in \mathbb{C} : \omega \in \Lambda(\mathcal{L} + \mathcal{E}) \text{ for some } \mathcal{E} \text{ with } \|\mathcal{E}\| \leq \epsilon\}.$$

In words, the ϵ-pseudospectrum of $\mathcal{L}$ is the union of the spectra of all perturbed operators $\mathcal{L} + \mathcal{E}$ with $\|\mathcal{E}\| \leq \epsilon$, together with any limit points of this set (a technicality of little importance). It is interesting to reconsider the implications of Figs. 4 and 5 in the light of this alternative characterization. The pseudospectral boundary contours in these figures imply that although the flows in question are eigenvalue stable (for $R < 5772$ in the Poiseuille case), exceedingly
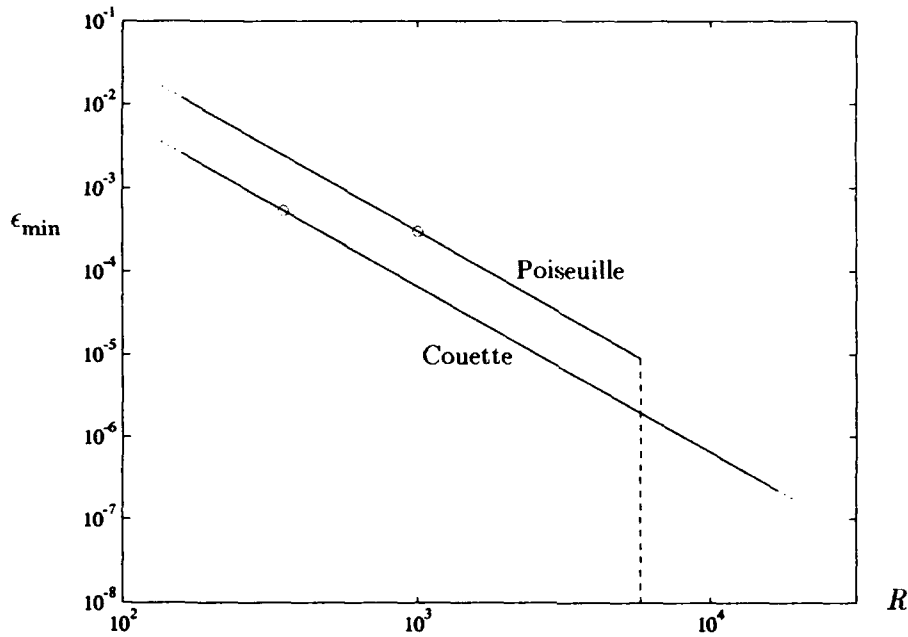
Fig. 12. An eigenvalue stable shear flow at Reynolds number R can be destabilized by a linear operator perturbation $\mathcal{E}$ of norm $\epsilon_{min} = O(R^{-2})$: the dependence is so nearly quadratic that the curves appear straight to plotting accuracy. The inverse $\epsilon_{min}^{-1} = O(R^2)$ is equal to the maximal resonant amplification plotted in Fig. 2. The circles mark the approximate Reynolds numbers (350, 1000) at which Couette and Poiseuille flows are observed to undergo transition to turbulence.

small perturbations to the evolution operator, of order $O(R^{-2})$, suffice to make them eigenvalue unstable. The norm of the minimal destabilizing perturbation is $\epsilon_{min} = (\sup_{\omega \in \mathbb{R}} \|(\omega I - \mathcal{L})^{-1}\|)^{-1}$, i.e., the inverse of the quantity plotted in Fig. 2 and labeled maximal resonance in Table 1. This observation provides a new interpretation of Fig. 2. For example, although Poiseuille flow with $R = 5000$ is eigenvalue stable, there exists a perturbation $\mathcal{E}$ of norm 1.21×10^{-5} that renders it unstable. See Fig. 12.

This raises the question of the physical meaning of operator perturbations and what relevance they may have to flow instabilities observed in the laboratory. (We emphasize that $\mathcal{E}$ is a perturbation of $\mathcal{L}$, not of the flow field u_0.) The minimal destabilizing perturbation $\mathcal{E}$ with $\|\mathcal{E}\| = \epsilon_{min}$ is easily characterized: it is a rank-1 operator of the form $\sigma v u^*$, where σ, v, u are the principal singular value and right and left singular vectors of $\mathcal{L}^{-1}$, respectively. This operator transforms streamwise streaks into streamwise vortices, thereby closing

the loop so that the transient growth of Figs. 8-9 can feed back upon itself to become modal growth for all t. Of course there is no reason to expect such a perfectly contrived perturbation to arise under natural conditions. What is suggestive is that even random perturbations of $\mathcal{L}$ have qualitatively the same effect. At $R = 5000$, for example, approximately 90% of all random perturbations $\mathcal{E}$ to $\mathcal{L}$ with $\|\mathcal{E}\| = 10^{-3}$ render a Poiseuille flow eigenvalue unstable, where by a random perturbation we mean an elementwise random perturbation of the 20×20 matrix that represents the projection of $\mathcal{L}$ onto the space spanned by its 20 dominant eigenmodes (with fixed $\alpha = 0$ and $\beta = 1.62$). Though it is a large step from such matrices to shear flows, the possibility is clearly suggested that seemingly negligible perturbations may destabilize a flow even in the narrow eigenvalue sense. One can imagine that imperfections in the boundary walls of a laboratory apparatus, for example, might have this effect. We hope that future investigations will reveal whether this idea of perturbed evolution operators provides an explanation of instability in some flows.

A different prospective application of the idea of destabilizing operator perturbations may be to the theory of "secondary instability" as an explanation of subcritical transition to turbulence (8, 9). This theory is founded on the discovery that when certain laminar shear flows are perturbed by certain physically motivated waves of large amplitude, the resulting problem is eigenvalue unstable, with eigenvalues high enough in the upper half-plane to match observed time scales for transition. The great sensitivity of the spectrum of $\mathcal{L}$ to perturbations, however, raises the question of whether similar eigenvalue instabilities might also arise with the use of more or less arbitrary perturbations, not just the ones that have been considered based on physical arguments.

Nonlinear bootstrapping and transition to turbulence

Kelvin wrote in 1887 (19):

It seems probable, almost certain indeed, that... the steady motion is stable for any viscosity, however small; and that the practical unsteadiness pointed out by Stokes forty-four years ago, and so admirably investigated experimentally five or six years ago by Osborne Reynolds, is to be explained by limits of stability becoming narrower and narrower the smaller is the viscosity.

This view of instability is still the standard one, but to this day, it has never been confirmed in detail. In this final section we would like to speculate about what the eventual confirmation may look like—in other words, about how nonlinear and linear mechanisms interact to bring about transition to turbulence.

Consider the 2×2 nonlinear model problem

$$\frac{du}{dt} = Au + \|u\|Bu, \qquad A = \begin{pmatrix} -R^{-1} & 1 \\ 0 & -2R^{-1} \end{pmatrix}, \qquad B = \begin{pmatrix} 0 & -1 \\ 1 & 0 \end{pmatrix},$$

where R is a large parameter. The linear term, involving the non-normal matrix A, amplifies energy transiently. The nonlinear term, involving the skew-symmetric matrix B, rotates energy in the u_1-u_2 plane but does not directly create or destroy energy, since it acts orthogonally to the motion (43). Thus we have linear amplification coupled with energy-neutral nonlinear mixing, a situation that holds also for the equations of fluid mechanics (44).

Fig. 13 shows norms $\|u(t)\|$ for solutions starting from eight different initial vectors of the form $u(0) = (0, \text{const})^T$, with $R = 25$. For $\|u(0)\| \leq 10^{-4}$, the curves are approximately translates of one another on this log scale, indicating that the evolution is effectively linear. At $\|u(0)\| = 4 \times 10^{-4}$, the nonlinearity has begun to have a pronounced effect. At $\|u(0)\| = 5 \times 10^{-4}$ the threshold has been crossed, and for this and higher amplitudes, the curves do not decay to zero but blow up to a critical point of amplitude ≈ 1.

Fig. 13 reveals a remarkable phenomenon: the amplitude growth is far greater than that of the purely linear problem $du/dt = Au$. Table 2 lists the linear growth factor $M \sim R/4$ and the threshold amplitude ϵ (for this particular choice of initial vector) for four values of R. Evidently ϵ is of order M^{-3}, not M^{-1}. This "bootstrapping" effect can be explained as follows. Suppose the solution at $t = 0$ consists of a vector of amplitude ϵ in a direction that excites
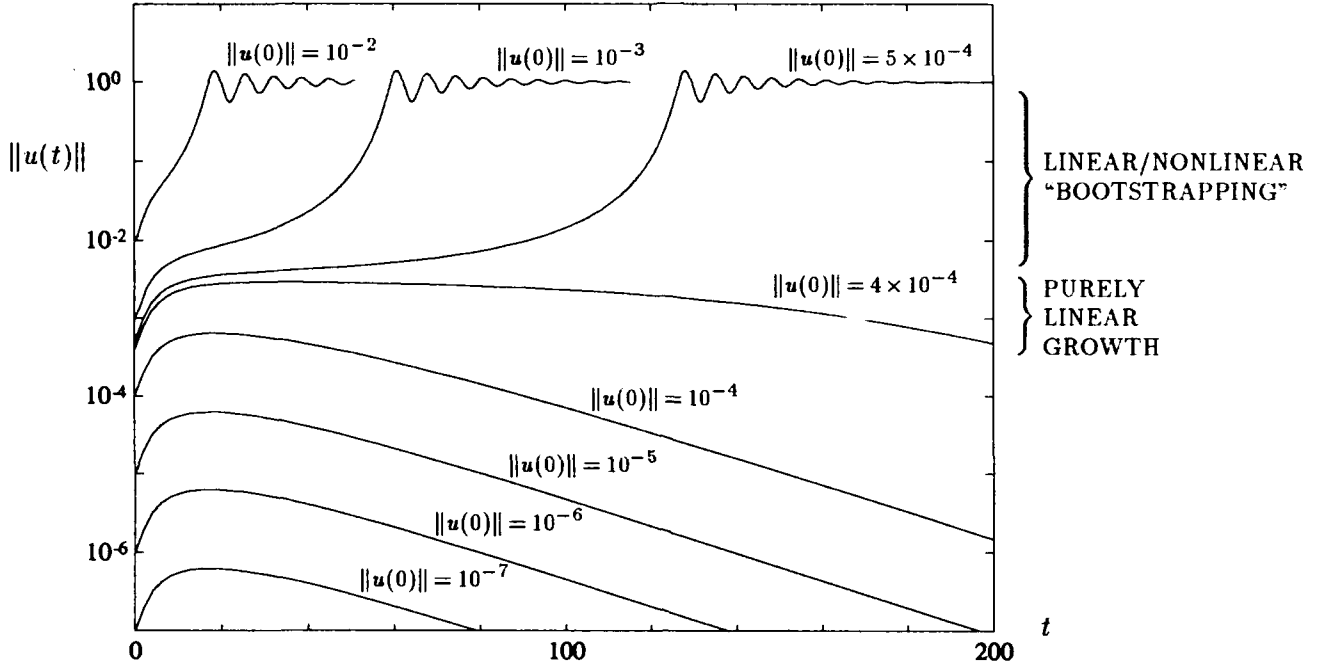
Fig. 13. $\|u(t)\|$ vs. t for solutions to a nonlinear 2×2 model problem with various initial amplitudes. The threshold amplitude is $\|u(0)\| \approx 4.22\times10^{-5}$.

R	linear growth factor M	threshold amplitude ϵ	ratio
12.5	3.18	3.41×10^{-3}	
25	6.28	4.22×10^{-4}	8.1
50	12.5	5.27×10^{-5}	8.0
100	25.0	6.58×10^{-6}	8.0

Table 2. The "bootstrapping" of the linear growth factor $M = O(R)$ causes the threshold amplitude to be $O(R^{-3})$.

growth of the linear problem $du/dt = Au$ (the principal right singular vector of A). At a later time, of order R, the solution has grown to order $R\epsilon$ by the linear growth mechanism but moved into a direction that no longer excites growth (the corresponding left singular vector). Meanwhile, however, the nonlinear term has had the effect of transferring some of this energy back to the original direction,

with amplitude $R(R\epsilon)^2 = R^3\epsilon^2$ since the nonlinearity is quadratic and the time scale is $O(R)$. If $R^3\epsilon^2$ is of order less than ϵ, the process is not self-sustaining and the energy dies away. On the other hand if $R^3\epsilon^2$ is of order greater than ϵ, then there is more energy than was present at the start and feedback occurs, leading to self-sustained amplitude growth. Thus the threshold amplitude is $\epsilon = O(R^{-3})$.

A similar experiment shows that if the same nonlinear equation is driven by a forcing oscillation $e^{i\omega t}v$ instead of an initial vector $u(0)$, the threshold amplitude becomes $\epsilon = O(R^{-4})$.

It may appear at first sight that these results indicate the great power and importance of nonlinear effects. Yet in two senses, these energy growth scenarios are essentially linear. First, as mentioned above, the nonlinear term does not add energy locally but merely redistributes it. Second, the appearance of the bootstrapping phenomenon does not depend on the precise nature of the nonlinearity. Any quadratic nonlinear term that transfers energy from decaying to growing solution components has the potential of inducing a threshold amplitude $\epsilon = O(R^{-3})$ or $O(R^{-4})$ with respect to initial or forcing data, respectively; a random perturbation, for example, will often suffice. Higher-order nonlinearities also lead to similar effects, though the exponents may be lowered, e.g. to $\epsilon = O(R^{-2})$ and $O(R^{-3})$ for a cubic nonlinearity.

The Navier-Stokes equations are certainly more complicated than our 2×2 model. One difference is that instead of 2-vectors, they act on functions with infinitely many degrees of freedom, most of which do not experience non-normal linear growth. There will always be some energy in the growing pseudomodes, however, and in a pipe or channel of substantial extent, random fluctuations can be expected to raise the energy levels in such components locally well about the statistical average (45, 46). Another difference is that the nonlinear interactions in the Navier-Stokes equations act across different wave numbers α and β (13, 14), making the exponent of 2 in our model perhaps unrealistically low. Despite these qualifications, we conjecture that the transition to turbulence of eigenvalue-stable shear flows proceeds analogously to our model in that the destabilizing mechanism is essentially linear in the senses described above, with an amplitude threshold for transition of order $O(R^\alpha)$ for some $\alpha < -1$.

Conclusion

In this article we have described three essentially linear approaches to the phenomenon of instability of shear flows: *(i)* (pseudo-) resonance, *(ii)* transient energy growth, and *(iii)* destabilizing operator perturbations. These ideas are by no means independent. Mathematically, they are all related to the pseudospectra of the operator $\mathcal{L}$, and physically, they all depend on the same mechanisms of extraction of energy from the mean flow by streamwise vortices and other structures. One should not expect that any one of these ideas will necessarily prove to be the "right" one, but rather, that each of them may prove appropriate to a particular class of experiments. For example, it is reasonable to speculate that in different situations transition to turbulence may be primarily triggered in physically quite different ways by *(i)* laboratory vibrations, *(ii)* initial or inlet disturbances, or *(iii)* deviations of the pipe or channel geometry from the Poiseuille or Couette ideal.

It is likely that in the upcoming decade, great progress will be made in elucidating these details. Numerical simulations of the 3D Navier-Stokes equations are becoming routine, and in the next few years such simulations will probably settle at last the question mentioned in the last section, for example, of how the threshold amplitude for transition depends on the Reynolds number in various flow situations.

Besides hydrodynamic stability, there are other fields also where highly non-orthogonal eigenfunctions arise and eigenvalues may be misleading. Examples in fluid mechanics include the instability of magnetic plasmas (48) and the formation of cyclones (49). Two more examples come from the field of numerical analysis: the numerical instability of discretizations of differential equations (40) and the convergence of iterative algorithms for nonsymmetric systems of linear equations (50). The recurring theme in these and other applications is that although the long-time behavior of an evolving system may be controlled by nonlinearities, some important phenomena are of a short-time nature and essentially linear (51, 52). If the linearized problem is far from normal, eigenvalues may be precisely the wrong tool for analyzing it, for eigenvalues determine the long-time behavior of a non-normal linear process, not the transient. We can expect to see further examples of alternatives to eigenvalues in the years ahead.

REFERENCES AND NOTES

1. P. G. Drazin and W. H. Reid, *Hydrodynamic Stability* (Cambridge U. Press, 1981).

2. D. D. Joseph, *Stability of Fluid Motions I* (Springer Verlag, 1975).

3. This article is adapted from L. N. Trefethen, A. E. Trefethen, S. C. Reddy, Technical Report No. TR 92-1291 (Department of Computer Science, Cornell University, 1992). Readers interested in additional details are urged to contact the first author for a copy of this report.

4. The Reynolds number is defined by $R = L V \rho / \mu$, where L is the half-width of the channel, V is the maximum velocity, ρ is the density, and μ is the viscosity. The distance, velocity, and time variables in our equations are nondimensionalized by L, V, and L/V, respectively.

5. S. A. Orszag, *J. Fluid Mech.* **50**, 689 (1971).

6. S. J. Davies and C. M. White, *Proc. Roy. Soc. A* **119**, 92 (1928); V. Patel and M. R. Head, *J. Fluid Mech.* **38**, 181 (1969); D. R. Carlson, S. E. Widnall, and M. F. Peeters, *ibid.* **121**, 487 (1982).

7. N. Tillmark and P. H. Alfredsson, J. Fluid Mech. **235**, 89 (1992).

8. S. A. Orszag and A. T. Patera, *J. Fluid Mech.* **128**, 347 (1983).

9. B. J. Bayly, S. A. Orszag, T. Herbert, *Ann. Rev. Fluid Mech.* **20**, 359 (1988).

10. T. Kato, *Perturbation Theory for Linear Operators* (Springer-Verlag, 1976).

11. A. Pazy, *Semigroups of Linear Operators and Applications to Partial Differential Equations* (Springer-Verlag, 1983).

12. S. C. Reddy, P. J. Schmid, D. S. Henningson, *SIAM J. Appl. Math.* **53**, in press.

13. L. H. Gustavsson, *J. Fluid Mech.* **224**, 241 (1991).

14. D. S. Henningson, in *Advances in Turbulence*, A. V. Johansson and P. H. Alfredsson Eds. (Springer-Verlag, 1991), pp. 279–284; D. S. Henningson, A. Lundbladh, A. V. Johansson, *J. Fluid Mech.*, in press.

15. K. M. Butler and B. F. Farrell, *Phys. Fluids A* **4**, 1637 (1992).

16. S. C. Reddy and D. S. Henningson, "Energy growth in viscous channel flows," to appear.

17. Closely related recent developments are described in K. S. Breuer and J. H. Haritonidis, *J. Fluid Mech.* **220**, 569 (1990) and Y. Bun and W. O. Criminale, "Evolution of three dimensional disturbances in a mixing layer," submitted.

18. See, e.g., Figs. 4.11, 4.15, 5.5 of (1). To be precise, the figures that have appeared in the literature have the x wavenumber α as the ordinate, not the x-z wave number magnitude $k = (\alpha^2 + \beta^2)^{1/2}$, and thus correspond to 2D perturbations only. This changes the upper boundary in such a way that the black region shrinks to zero width as $R \rightarrow \infty$.

19. Lord Kelvin (W. Thomson), *Phil. Mag.* **24**, 188 (1887).

20. W. M'F. Orr, *Proc. Roy. Irish Acad. A* **27**, 9 and 69 (1907).

21. K. M. Case, *J. Fluid Mech.* **10**, 420 (1960) and *Phys. Fluids* **3**, 143 (1960).

22. G. Rosen, *Phys. Fluids* **14**, 2767 (1971); D. J. Benney and L. H. Gustavsson, *Stud. Appl. Math.* **64**, 185 (1981); L. S. Hultgren and L. H. Gustavsson, *Phys. Fluids* **24**, 1000 (1981), B. F. Farrell, *ibid.* **31**, 2093 (1988).

23. A. D. D. Craik and W. O. Criminale, *Proc. Roy. Soc. A* **406**, 13 (1986).

24. H. B. Squire, *Proc. Roy. Soc. A* **142**, 621 (1933).

25. P. S. Klebanoff, K. D. Tidstrom, L. M. Sargent, *J. Fluid Mech.* **12**, 1 (1962); R. Breidenthal, *ibid.* **109**, 1 (1981); L. P. Bernal and A. Roshko, *ibid.* **170**, 499 (1986); J. C. Lasheras and H. Choi, *ibid.* **189**, 53 (1988); M. Asai and M. Nishioka, *ibid.* **208**, 1 (1989); S. K. Robinson, Tech. Memo. NASA TM-103859, NASA, 1991.

26. This process is sometimes called "lift-up;" see M. T. Landahl, *SIAM J. Appl. Math.* **28**, 735 (1975).

27. The term pseudospectrum is due to L. N. Trefethen; see e.g. L. N. Trefethen, in *Numerical Analysis 1991*, D. F. Griffiths and G. A. Watson Eds. (Longman, 1992), pp. 234-266. Essentially the same idea has been applied over the years by various authors including J. M. Varah, J. W. Demmel, and especially S. K. Godunov and his colleagues in the former Soviet Union. Perhaps its earliest application is by H. J. Landau, *J. Opt. Soc. Am.* **66**, 525 (1976).

28. Our computations have been carried out on a Connection Machine System CM-5 in Fortran and on Sun workstations in Matlab, using numerical methods adapted from those of Reddy and Henningson (12, 13, 14, 16). First the problem is Fourier transformed in x and z, and the working variables are taken as the y components of velocity and vorticity; a weighted norm is introduced for these variables that is equivalent to the energy norm $\| \cdot \|$. The 1D problem is discretized by a Chebyshev hybrid spectral method and then projected onto a space spanned by a set of dominant eigenmodes, leading to matrices typically of size about 80×80. In the Poiseuille case the odd and even solutions with respect to y decouple, and we take advantage of this separation. The generation of most of our figures requires an optimization with respect to α or β or both. The largest calculations are required for the pseudospectra of Figs. 4 and 5, which are determined by evaluating $\|(\omega I - \mathcal{L})^{-1}\|$ on a grid in the ω-plane of typical size 64×64 and plotting contours of the resulting data array. For each value of ω on the grid, $\|(\omega I - \mathcal{L})^{-1}\|$ is computed by numerical minimization of $\|(\omega I - \mathcal{L}_{\alpha\beta})^{-1}\|^{-1}$ with respect to α and β, and each evaluation of this function entails a matrix singular value decomposition (SVD).

29. L. M. Mack, *J. Fluid Mech.* **73**, 497 (1976).

30. The principal difference is that the spectra and pseudospectra are broader in Fig. 5 than in Fig. 4. This is a consequence of the fact that the mean flow velocity is zero for Couette flow but nonzero for Poiseuille flow, so that a plane wave of wavenumber α traveling with the mean flow will have $\omega \approx 0$ for Couette flow but $\omega = O(\alpha)$ for Poiseuille flow. Figs. 4 and 5 look different if the Navier-Stokes problem is formulated in a moving reference frame, though the behavior along the imaginary axis is essentially unchanged.

31. The angle is $\theta \approx 16.4°$ as measured in the energy inner product, corresponding to an eigenvalue condition number $\kappa = 1/\sin\theta \approx 3.52$. Thus the small bump in the $\epsilon = 10^{-3.5}$ pseudospectral contour of Fig. 5b lies at a distance $3.52 \times 10^{-3.5}$ from the spectrum.

32. Similar figures appear in (15). Detailed discussions of the differences between structures with $\alpha = 0$, $\alpha \neq 0$, etc. can be found there and in B. F. Farrell and P. J. Ioannou, "Optimal excitation of 3D perturbations in viscous constant shear flow," to appear. In the present paper we have oversimplified somewhat by emphasizing only streamwise structures.

33. This figure is modeled after Fig. 13 of (12), an analogous plot for 2D perturbations only.

34. It has been conjectured that the pseudospectra of a matrix or linear operator $\mathcal{L}$ determine $\|\exp(-it\mathcal{L})\|$ and indeed any quantity $\|f(\mathcal{L})\|$ exactly, not just approximately via inequalities (A. Greenbaum and L. N. Trefethen, "GMRES/CR and Arnoldi/Lanczos as matrix approximation problems," to appear). As of this writing, the validity of this conjecture is unresolved.

35. G. H. Golub and C. F. Van Loan, *Matrix Computations* (Johns Hopkins U. Press, 1989); R. A. Horn and C. R. Johnson, *Topics in Matrix Analysis* (Cambridge U. Press, 1991).

36. J. Serrin, *Arch. Rat. Mech. Anal.* **3**, 1 (1959); F. H. Busse, *Z. Angew. Math. Phys.* **20**, 1 (1969); J. L. Lumley, in *Developments in Mechanics, Vol. 6*, L. H. N. Lee and A. H. Szewczyk Eds. (Notre Dame Press, 1971), pp. 63-88.

37. Lord Rayleigh, *Proc. London Math. Soc.* **11**, 57 (1880).

38. T. Ellingsen and E. Palm, *Phys. Fluids* **18**, 487 (1975).

39. M. T. Landahl, *J. Fluid Mech.* **98**, 243 (1980).

40. This point has been better appreciated in the field of numerical analysis of discrete methods for the solution of differential equations. The proper definition of numerical stability, due to P. D. Lax and R. D. Richtmyer, is uniform with respect to a mesh size parameter, and the importance of uniform estimates was made especially clear by the work of H.-O. Kreiss in the 1960s. See (42) and R. D. Richtmyer and K. W. Morton, *Difference Methods for Initial-Value Problems* (Wiley-Interscience, 1967).

41. The spectrum $\Lambda(\mathcal{L})$ and pseudospectra $\Lambda_\epsilon(\mathcal{L})$ are discontinuous as $R \to \infty$: for both Couette and Poiseuille flow with $R = \infty$ the spectrum is the real axis, not the lower half-plane, and preliminary results suggest that the pseudospectra are approximately parallel strips centered on the real axis. (The $\pm i$ symmetry is a consequence of the reversibility of inviscid flows.) These discontinuities do not reflect any genuine difficulty with the limit $R \to \infty$, however, for it is only the pseudospectra in the upper half-plane that have quantitative consequences, and these, so far as we know, are continuous.

42. S. C. Reddy and L. N. Trefethen, *Numer. Math.* **62**, 236 (1992).

43. The fact that the nonlinear term does not create or destroy energy can be seen algebraically from the absence of B from the easily verified formula $d\|u\|^2/dt = u^T(A + A^T)u$.

44. The equation for $d\|u\|^2/dt$ is called the Reynolds-Orr equation (1,2). In fact our 2×2 model is not so far from the interaction of vortex "tilting" and "stretching" described in (8), p. 369.

45. We have not discussed the relationship between spatially global and local results, which is somewhat obscured by modal or pseudomodal analysis, since different wave numbers α, β decouple orthogonally. A related matter is the investigation of spatial rather than temporal evolution of flow disturbances, which, according to preliminary results of P. J. Schmid (personal communication), produces results qualitatively analogous to those reported here.

46. Preliminary numerical experiments support the idea that even random fluctuations tend to excite growing pseudomodes. A theory of the non-normal response of linearized flows to stochastic forcing data has been developed in B. F. Farrell and P. J. Ioannou, "Stochastic forcing of the linearized Navier-Stokes equations," to appear. In the language of numerical linear algebra, this work is related to the integral of the squared Frobenius norm of the evolution operator $\exp(-it\mathcal{L})$ (sum of squares of all singular values) rather than the energy norm (largest singular value).

47. P. J. Schmid and D. S. Henningson, *Phys. Fluids A* **4**, 1986 (1992).

48. W. Kerner, *J. Comp. Phys.* **85**, 1 (1989).

49. B. F. Farrell, *J. Atmos. Sci.* **46**, 1193 (1989).

50. N. M. Nachtigal, S. C. Reddy, L. N. Trefethen, *SIAM J. Matrix Anal. Appl.* **13**, 778 (1992); N. M. Nachtigal, L. Reichel, L. N. Trefethen, *ibid.*, 796.

51. D. J. Higham and L. N. Trefethen, "Stiffness of ODEs," *BIT*, in press.

52. There is evidence that this statement applies even to fully developed turbulence. See M. J. Lee, J. Kim, P. Moin, *J. Fluid Mech.* **216**, 561 (1990) and K. M. Butler and B. F. Farrell, "Optimal perturbations and streak spacing in wall-bounded turbulent shear flow," *Phys. Fluids A*, in press.

53. Supported by NSF Grant DMS-9116110 (L.N.T). We acknowledge with gratitude the comments of Kathryn Butler, Brian Farrell, Bengt Fornberg, Dan Henningson, Philip Holmes, Petros Ioannou, Peter Schmid, Ridgway Scott, and Eric Siggia, and also extensive CM-5 computer time generously donated by Thinking Machines Corporation.

REPORT DOCUMENTATION PAGE

Public reporting burden for this collection of information is estimated to average 1 hour per response, including the time for reviewing instructions, searching existing data sources, gathering and maintaining the data needed, and completing and reviewing the collection of information. Send comments regarding this burden estimate or any other aspect of this collection of information, including suggestions for reducing this burden, to Washington Headquarters Services, Directorate for information Operations and Reports, 1215 Jefferson Davis Highway, Suite 1204, Arlington, VA 22202-4302, and to the Office of Management and Budget, Paperwork Reduction Project (0704-0188), Washington, DC 20503

1. AGENCY USE ONLY (Leave blank)	2. REPORT DATE December 1992	3. REPORT TYPE AND DATES COVERED Contractor Report

4. TITLE AND SUBTITLE

A NEW DIRECTION IN HYDRODYNAMIC STABILITY: BEYOND EIGENVALUES

5. FUNDING NUMBERS

C NAS1-19480

WU 505-90-52-01

6. AUTHOR(S)

Lloyd N. Trefethen, Anne E. Trefethen, Satish C. Reddy, and Tobin A. Driscoll

7. PERFORMING ORGANIZATION NAME(S) AND ADDRESS(ES)

Institute for Computer Applications in Science
 and Engineering
Mail Stop 132C, NASA Langley Research Center
Hampton, VA 23681-0001

8. PERFORMING ORGANIZATION REPORT NUMBER

ICASE Report No. 92-71

9. SPONSORING/MONITORING AGENCY NAME(S) AND ADDRESS(ES)

National Aeronautics and Space Administration
Langley Research Center
Hampton, VA 23681-0001

10. SPONSORING/MONITORING AGENCY REPORT NUMBER

NASA CR-191411
ICASE Report No. 92-71

11. SUPPLEMENTARY NOTES

Submitted to Science

Langley Technical Monitor: Michael F. Card
Final Report

12a. DISTRIBUTION/AVAILABILITY STATEMENT

Unclassified - Unlimited
Subject Category 34

12b. DISTRIBUTION CODE

13. ABSTRACT (Maximum 200 words)

Fluid flows that are smooth at low speeds become unstable and then turbulent at higher speeds. This phenomenon has traditionally been investigated by linearizing the equations of flow and looking for unstable eigenvalues of the linearized problem, but the results agree poorly in many cases with experiments. Nevertheless, it has become clear in recent years that linear effects play a central role in hydrodynamic instability. A reconciliation of these findings with the traditional analysis can be obtained by considering the "pseudospectra" of the linearized problem, which reveals that small perturbations to the smooth flow in the form of streamwise vortices may be amplified by factors on the order of 10^5 by a linear mechanism, even though all the eigenmodes are stable. The same principles apply also to other problems in the mathematical sciences that involve non-orthogonal eigenfunctions.

14. SUBJECT TERMS

hydrodynamic stability; transition to turbulence

15. NUMBER OF PAGES

31

16. PRICE CODE

A03

17. SECURITY CLASSIFICATION OF REPORT	18. SECURITY CLASSIFICATION OF THIS PAGE	19. SECURITY CLASSIFICATION OF ABSTRACT	20. LIMITATION OF ABSTRACT
Unclassified	Unclassified		

NSN 7540-01-280-5500

National Aeronautics and
Space Administration
Code JTT
Washington, D.C.
20546-0001
Official Business
Penalty for Private Use, $300

NASA

POSTMASTER: If Undeliverable (Section 158
                Postal Manual) Do Not Return